

Evidence for a direct band gap in the topological insulator Bi_2Se_3 from theory and experiment

I. A. Nechaev,^{1,2} R. C. Hatch,³ M. Bianchi,³ D. Guan,³ C. Friedrich,⁴ I. Aguilera,⁴
J. L. Mi,⁵ B. B. Iversen,⁵ S. Blügel,⁴ Ph. Hofmann,³ and E. V. Chulkov^{2,6,7}

¹*Tomsk State University, 634050, Tomsk, Russia*

²*Donostia International Physics Center (DIPC),*

20018 San Sebastián/Donostia, Basque Country, Spain

³*Department of Physics and Astronomy, Interdisciplinary Nanoscience Center, Aarhus University, 8000 Aarhus C, Denmark*

⁴*Peter Grünberg Institut and Institute for Advanced Simulation,
Forschungszentrum Jülich and JARA, D-52425 Jülich, Germany*

⁵*Center for Materials Crystallography, Department of Chemistry,
Interdisciplinary Nanoscience Center, Aarhus University, 8000 Aarhus C, Denmark*

⁶*Departamento de Física de Materiales UPV/EHU,
Facultad de Ciencias Químicas, UPV/EHU, Apdo. 1072,
20080 San Sebastián/Donostia, Basque Country, Spain*

⁷*Centro de Física de Materiales CFM - MPC, Centro Mixto CSIC-UPV/EHU,
20080 San Sebastián/Donostia, Basque Country, Spain*

(Dated: October 17, 2012)

Using angle-resolved photoelectron spectroscopy and *ab-initio* *GW* calculations, we unambiguously show that the widely investigated three-dimensional topological insulator Bi_2Se_3 has a direct band gap at the Γ point. Experimentally, this is shown by a three-dimensional band mapping in large fractions of the Brillouin zone. Theoretically, we demonstrate that the valence band maximum is located at the Brillouin center only if many-body effects are included in the calculation. Otherwise, it is found in a high-symmetry mirror plane away from the zone center.

PACS numbers: 71.15.m, 71.20.b, 71.70.Ej, 79.60.-i

Bismuth selenide is a prototypical topological insulator (TI) that, after its identification as such a material [1, 2], has been very widely studied. Its surface electronic structure consists of a single Dirac cone around the surface Brillouin zone (SBZ) centre $\bar{\Gamma}$, with the Dirac point (DP) placed closely above the bulk valence band states. In order to exploit the multitude of interesting phenomena associated with the topological surface states [3, 4], it is necessary to access the topological transport regime with the chemical potential near the DP, but simultaneously in the absolute bulk band gap. Due to the close proximity of the DP and the bulk valence states at $\bar{\Gamma}$, this is only possible if there are no other valence states in Bi_2Se_3 with energies close to or higher than the DP. As the bulk conduction band minimum (CBM) is undisputedly placed at Γ (see, e.g., Refs. 5 and 6), the question if the absolute valence band maximum is below the DP at Γ or at other locations in the Brillouin zone (BZ) is identical to the question about the nature of the fundamental band gap, direct or indirect.

The nature of the bulk band gap is thus of crucial importance for the possibility to exploit the topological surface states in transport but the position of the VBM in band structure calculations remains disputed. In a linearized muffin-tin orbital method (LMTO) calculation within the local density approximation (LDA), the VBM was found at the Γ point, implying that Bi_2Se_3 is a direct-gap semiconductor [7]. Contrarily, by employing the full-potential linearized augmented-plane-wave

method (FLAPW) within the generalized gradient approximation (GGA), the authors of Ref. 5 have found the VBM to be located on the $Z - F$ line of the BZ, which is lying in the mirror plane. Similar results have been obtained in Ref. 8 with the plane-wave pseudopotential method (PWP) within the LDA. Various density functional theory (DFT) calculations of the surface band structure of Bi_2Se_3 [1, 3, 9, 10] also indicate that the VBM of bulk bismuth selenide is not located at the BZ center. In these calculations the projected bulk states show the VBM to lie on the $\bar{\Gamma} - \bar{M}$ direction of the SBZ. A shift of the VBM towards the Γ point caused by taking into account many-body corrections within the *GW* approximation was demonstrated in Ref. 8. So far, however, the valence band dispersion has only been calculated along high-symmetry lines of the BZ, precluding a firm conclusion about the position of the VBM in the three-dimensional BZ. Thus, the nature of the band gap has not been determined unequivocally so far.

Experimentally, it appears that the assumption that bismuth selenide is a material with a direct band gap has first been made in Ref. 11, where galvanomagnetic properties were investigated. By inspecting angle-resolved photoemission spectra in the $\Gamma - Z - F$ direction, the authors of Ref. 5 have concluded that the VBM is located at the Γ point. More recent experimental evidence appears to support this but most studies have focused on the topological state in the immediate vicinity of $\bar{\Gamma}$ (see e.g. Ref. 2). Even if a systematic exploration of

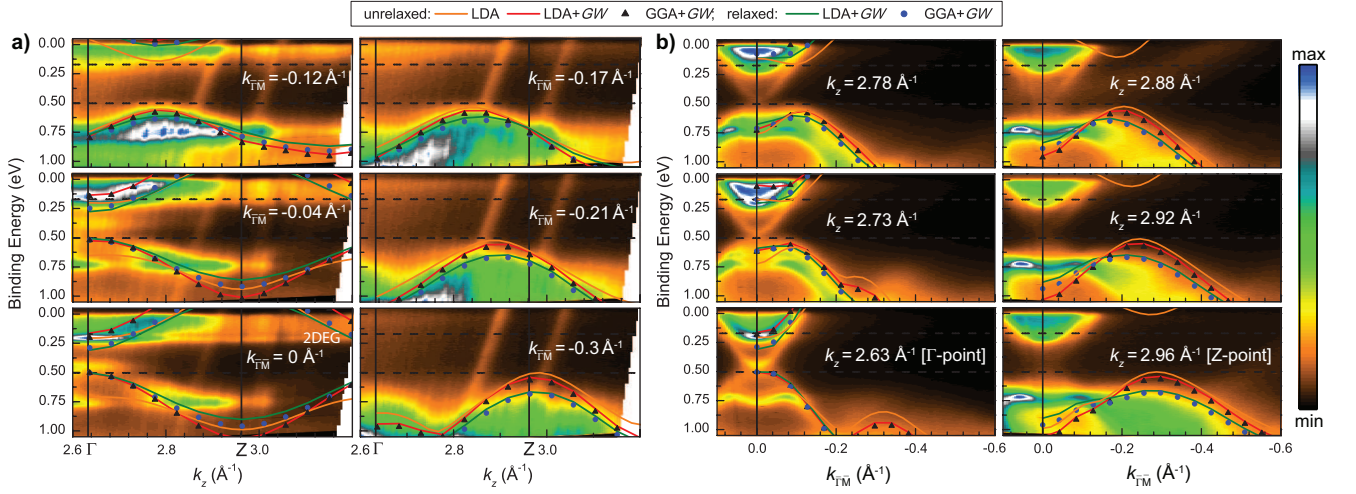


FIG. 1: (Color online) Photoemission intensity and theoretical results at different constant parallel momenta $k_{\Gamma\bar{M}}$ along directions parallel to $\Gamma - Z$ (a) and normal momenta k_z along directions parallel to $Z - U$ (b), which are shown by vertical and horizontal dashed lines in Fig. 2, respectively. Dashed horizontal lines correspond to the experimentally observed energies of the VBM (0.505 ± 0.030 eV) and the CBM (0.170 ± 0.025 eV). The theoretical curves (shifted to have the VBM at the same energy as in the ARPES experiment) present the lowest conduction band and the uppermost valence band obtained for the experimental [12] (unrelaxed) and relaxed atomic positions without (LDA) and with (LDA+GW or GGA+GW) the GW corrections to the DFT (LDA or GGA) band structure. The two parallel and nearly vertical lines of higher photoemission intensity seen at k_z values of roughly 2.8 and 3.0 \AA^{-1} in Fig. (a) correspond to Bi 5d core levels which have been excited by second-order light from the monochromator.

the experimental dispersion along the $\bar{\Gamma} - \bar{M}$ is lacking, the existing evidence thus points towards a VBM at the Γ point, in contrast to most first-principle calculations that place the VBM quite far away from the Γ -point.

In this Letter, we report on theoretical and experimental evidence for a direct band gap in bismuth selenide. We systematically explore the valence band structure in large fractions of the BZ and show theoretically that the VBM is found at Γ , but only if GW corrections are taken into account. The calculated dispersion for the upper VB is found to be in good agreement with ARPES results. Our findings are important for the scattering and transport properties of the topological surface states and may call for a new interpretation of previous results in e.g. quasiparticle interference from these states, which involve the bulk band-structure features derived within the DFT [10].

Experiments were performed on single crystals of Bi_2Se_3 [14]. ARPES measurements were carried out on the SGM-3 beamline of the ASTRID synchrotron radiation facility [16]. In order to probe the Bi_2Se_3 bulk band structure, the photon energy was varied from 14 to 32 eV in 0.1 eV steps. The combined energy resolution was ≤ 22 meV and the angular resolution was $\sim 0.15^\circ$. Samples were cleaved *in-situ* at room temperature, then cooled to ~ 70 K for measurements. The k_z values for the three-dimensional representation of the photon energy scan were calculated using free-electron final states,

i.e., $k_z = \sqrt{2m_e/\hbar^2(V_0 + E_{\text{kin}} \cos^2(\theta))}^{1/2}$, where θ is the emission angle and V_0 is the inner potential. From the normal-emission ARPES data it is easy to locate a Γ point. The value of $V_0 = 11.8$ eV was determined by iteratively changing V_0 such that the k_z value corresponding to this Γ point agrees with the size of the Bi_2Se_3 BZ. It should be noted that $V_0 = 11.8$ eV is in good agreement with values reported previously [14, 15, 17, 18] and is the only value between 1 and 26 eV which results in a correct k_z value for the Γ point.

Experimentally, we go beyond the standard approach of ARPES band structure determinations by probing a large fraction of k -space on a dense grid of emission angles and photon energies, even though only a fraction of the data in the most relevant $\bar{\Gamma} - \bar{M}$ direction of the SBZ is shown here. Combined with the assumption of free electron final states, this permits us to plot the photoemission intensity as a function of k_z for a given $k_{\parallel} = k_{\Gamma\bar{M}}$ value parallel to the surface along $\bar{\Gamma} - \bar{M}$ [Fig. 1(a)] or at constant k_z as a function of $k_{\Gamma\bar{M}}$ [Fig. 1(b)]. This unconventional way of plotting ARPES results is only possible based on a large data set, but it is excellently suited for a comparison to band structure calculations.

Our *ab initio* calculations were performed by employing the FLAPW method as implemented in the FLEUR code [19] within both the LDA of Ref. 20 and the GGA of Ref. 21 for the exchange-correlation (XC) functional. The mentioned two approximations (LDA and GGA)

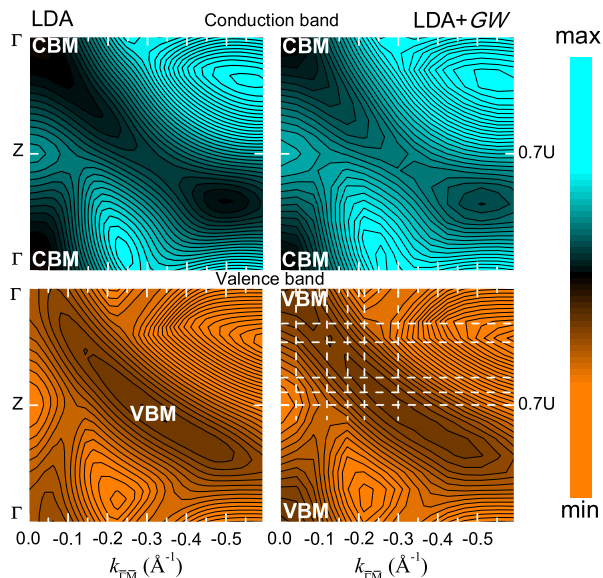


FIG. 2: (Color online) Contour plots of the lowest conduction band (upper row) and the uppermost valence band (lower row) in the mirror plane (see Fig. S1 of Supplemental Material [23]). The presented results are obtained for the experimental atomic positions without (LDA) and with (LDA+GW) the GW corrections to the LDA band structure. Vertical and horizontal dashed lines drawn on the valence-band contour plot in the LDA+GW case correspond to the cuts of the three-dimensional photon-energy scan, which are presented in Fig. 1.

have been used in order to reveal the effect of different reference one-particle band structures on the GW results. The GW approximation (with the inclusion of spin-orbit interaction as implemented in the SPEX code [13, 22]) was applied in the one-shot framework, where the Kohn-Sham eigenfunctions are taken as approximate quasiparticle wave functions. As an additional factor that can affect our *ab initio* results, we consider different atomic positions for Bi and Se atoms in a rhombohedral crystal structure with experimental lattice parameters taken from Ref. 12. One set of positions corresponds to the atomic positions reported in Ref. 12 (labeled as “unrelaxed”). Another set (labeled as “relaxed”) was obtained during a relaxation procedure optimizing the atomic positions at fixed volume. For more computational details, we refer the reader to Sec. S1 of the Supplemental Material [23].

It should be noted that our GW study goes beyond the one of Ref. 8 in several aspects: Instead of the PWP, we employ the FLAPW method, which treats core, valence, and conduction electrons on an equal footing. Furthermore, we do not resort to a plasmon-pole model for the dielectric matrix but use the random-phase approximation (RPA) explicitly without approximations for the frequency dependence. In Ref. 8 the GW calculation was

performed without spin-orbit coupling; spin-orbit interaction was included by second variation using the GW corrected eigenvalues only after the quasiparticle spectrum had been obtained. We use the full four-component spinor wave functions, as obtained from a fully relativistic DFT calculation, directly for the GW calculations as in Ref. 13. Spin off-diagonal elements in the Green function and the self-energy are thus fully taken into account. Finally, we investigate the behavior of the valence and conduction bands not only on certain lines of the BZ, but also in the whole symmetric mirror plane.

The calculations and ARPES results are compared in Fig. 1. The cut in Fig. 1(a) corresponding to $k_{\Gamma\bar{M}} = 0 \text{ \AA}^{-1}$, i.e., normal emission, has two features that disperse along k_z . These are derived from the CB and VB. The CB is partially occupied by the degenerate bulk doping of the sample. The data set also shows three features with non-dispersive two-dimensional (2D) character. The first one is the topological state at the Dirac point which is located at a binding energy of $E_B \approx 0.45 \text{ eV}$. The second and third features are the so-called M-shaped state at $E_B \approx 0.75 \text{ eV}$ and the parabolic free-electron-like state at $E_B \approx 0.25 \text{ eV}$ (the latter is indicated in Fig. 1(a) as 2DEG – two-dimensional electron gas). These states have been interpreted as the 2D states formed by the quantization of the valence and conduction band states, respectively, in a potential well formed by the downward bending of the bands at the surface [14, 24, 25]. Alternatively, in Refs. [26–29] the emergence of the states is explained by an expansion of van der Waals spacings due to intercalation of surface-deposited atoms. The intercalation of adsorbed Rb atoms, on the other hand, does not change the surface electronic structure significantly and so this point remains controversial [30]. The photoemission intensity of the surface-related features shows a resonant enhancement at the photon energies for which bulk states with a similar wave function periodicity along k_z is observed. The topological state and the 2D state in the conduction band are enhanced at Γ whereas the M-shaped state is enhanced near Z .

The best agreement between experimental and theoretical data is reached in the case of the LDA+GW calculations with the relaxed atomic positions. However, the experimental band-gap value ($0.332 \pm 0.055 \text{ eV}$) is not so well reproduced as in the LDA+GW case with experimental atomic positions (see Table I). As is clearly seen in Fig. 1(a), the shown LDA results, which reflect the situation when the VBM is located in the mirror plane of the BZ (see Fig. 2), are quite far from the experimentally observed valence-band edges. Also, it appears that all calculations overestimate the total width of the upper valence band.

Similar to the conventional semiconductor systems, the GW corrections to the LDA band structure have mainly “moved” the conduction band away from the valence

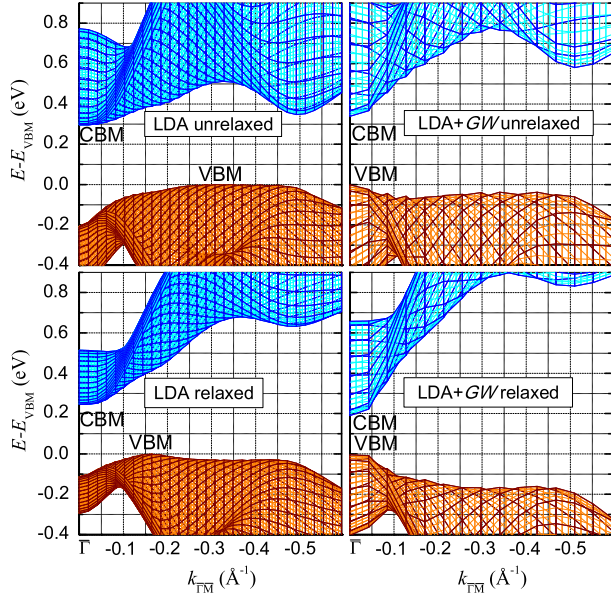


FIG. 3: (Color online) Projections of the lowest conduction band and the uppermost valence band in the mirror plane on the $\bar{\Gamma}-\bar{M}$ direction of the two-dimensional BZ. The presented results are obtained for the experimental (upper row) and relaxed (lower row) atomic positions without (LDA) and with (LDA+ GW) the GW corrections to the LDA band structure.

band on the energy scale. This fact is visually represented in Fig. 2, where one can catch sight of only slightly changed contours of the bands in the mirror plane upon including the many-body corrections. Nevertheless, there is a crucial point that drastically distinguishes the TI from the conventional semiconductors. This point is the band inversion near the center of the BZ. Owing to this inversion, as was recently shown in Ref. 8, the mentioned movement apart decreases the “penetration” of the bands into each other near the Γ point, i.e., the hybridization due to spin-orbit coupling is reduced, and, as a result, both the band-inversion region in k -space and the Γ -point band gap become smaller.

For bismuth selenide, the mentioned mechanism of the many-body corrections finally leads to shifting the VBM to the Γ point, as is clearly seen in Fig. 3, where an effect caused by the relaxation of the atomic positions is also shown. On the DFT level, the relaxation results in a shift of the VBM along the mirror plane towards the center of the BZ and a reduction of the indirect band gap. With the inclusion of the GW corrections, the relaxation causes a smaller direct band-gap value and a larger upward shift of the conduction band beyond the band-inversion region.

Fig. 4 shows the GGA band structure without and with the GW corrections. As compared to the LDA-based calculations, the presented data allow one to address the question of how different approximations to the XC functional affect the GW results. It is worth noting that we

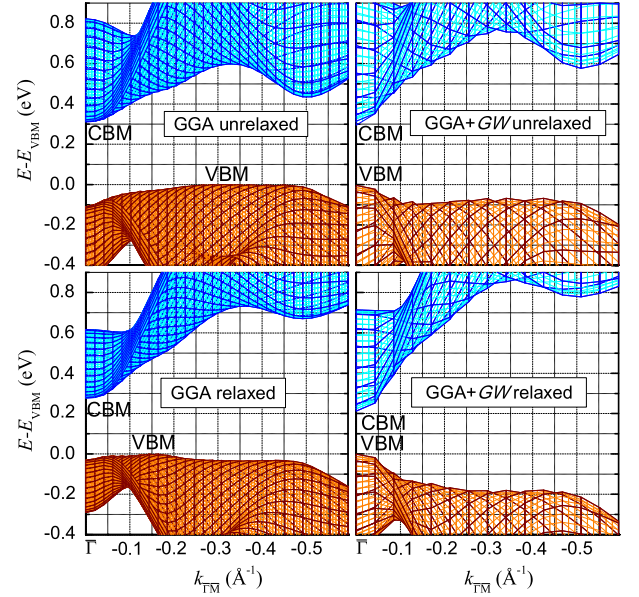


FIG. 4: (Color online) Same as in Fig. 3, but without (GGA) and with (GGA+ GW) the GW corrections to the GGA band structure.

TABLE I: The calculated band-gap values in eV for Bi_2Se_3 .

XC	type	unrelaxed	relaxed
LDA	indirect	0.30	0.25
LDA+ GW	direct	0.34	0.19
GGA	indirect	0.31	0.28
GGA+ GW	direct	0.30	0.21

have obtained not only similar behaviour of the bands under study for both reference band structures (LDA and GGA), but even qualitatively close GW -results on the valence-band edge, as one can judge from Fig. 1. Besides, the performed DFT+ GW calculations with different XC functionals and relaxed atomic positions give practically the same band-gap value (see Table I). Also, the RPA dielectric constant ϵ_∞ turns out to be quite stable upon changing the XC functional and relaxed atomic positions and is consistent with experimental data (see Table SI of Supplemental Material [23]).

In conclusion, we have presented ARPES measurements for bismuth selenide which are aimed at a study of the behaviour of the bulk valence-band in the high-symmetry mirror plane in the bulk BZ. We have probed a large range of k -space by taking data at a dense mesh of angles and photon energies (only data along $\bar{\Gamma}-\bar{M}$ shown here). We have theoretically considered the effect of many-body corrections within the GW approximation on the band structure, in particular, on the lowest conduction and highest valence band, and demonstrated how *ab initio* GW results depend on the DFT reference band structure and on atomic positions of Bi and Se atoms in

the rhombohedral crystal structure of Bi_2Se_3 . As a net result, we have arrived at theoretical and experimental data which are in good agreement and indicate consistently that Bi_2Se_3 is a direct-gap semiconductor with the VBM located at the Γ point.

-
- [1] H. Zhang, C.-X. Liu, X.-L. Qi, X. Dai, Z. Fang, and S.-C. Zhang, *Nat. Phys.* **5**, 438 (2009).
- [2] Y. Xia, D. Qian, D. Hsieh, L. Wray, A. Pal, H. Lin, A. Bansil, D. Grauer, Y. S. Hor, R. J. Cava, and M. Z. Hasan, *Nature Physics* **5**, 398 (2009).
- [3] D. Hsieh, Y. Xia, D. Qian, L. Wray, J.H. Dil, F. Meier, J. Osterwalder, L. Patthey, J.G. Checkelsky, N.P. Ong, A.V. Fedorov, H. Lin, A. Bansil, D. Grauer, Y.S. Hor, R.J. Cava, and M.Z. Hasan, *Nature* **460**, 1101 (2009).
- [4] M. Z. Hasan C. L. Kane, *Rev. Mod. Phys.* **82**, 3045 (2010).
- [5] V. A. Greanya, W. C. Tonjes, R. Liu, C. G. Olson, D.-Y. Chung, and M. G. Kanatzidis, *J. Appl. Phys.* **92**, 6658 (2002); P. Larson, V. A. Greanya, W. C. Tonjes, R. Liu, S. D. Mahanti, and C. G. Olson, *Phys. Rev. B* **65**, 085108 (2002).
- [6] Y. L. Chen, J.-H. Chu, J. G. Analytis, Z. K. Liu, K. Igarashi, H.-H. Kuo, X. L. Qi, S. K. Mo, R. G. Moore, D. H. Lu, M. Hashimoto, T. Sasagawa, S. C. Zhang, I. R. Fisher, Z. Hussain, and Z. X. Shen, *Science* **329**, 659 (2010).
- [7] S. K. Mishra, S. Satpathy, and O. Jepsen, *J. Phys.: Condens. Matter* **9**, 461 (1997).
- [8] O. V. Yazyev, E. Kioupakis, J. E. Moore, and S. G. Louie, *Phys. Rev. B* **85**, 161101(R) (2012).
- [9] S. V. Eremeev, Yu. M. Koroteev, and E. V. Chulkov, *JETP Letters*, **91**, 387 (2010).
- [10] S. Kim, M. Ye, K. Kuroda, Y. Yamada, E. E. Krasovskii, E. V. Chulkov, K. Miyamoto, M. Nakatake, T. Okuda, Y. Ueda, K. Shimada, H. Namatame, M. Taniguchi, and A. Kimura, *Phys. Rev. Lett.* **107**, 056803 (2011).
- [11] H. Köhler and A. Fabricius, *Phys. Stat. Sol. B* **71**, 487 (1975).
- [12] R.W.G. Wyckoff, *Crystal Structures* (J. Wiley and Sons, New York, 1964), Vol. 2.
- [13] R. Sakuma, C. Friedrich, T. Miyake, S. Blügel, and F. Aryasetiawan, *Phys. Rev. B* **84**, 085144 (2011).
- [14] M. Bianchi, D. Guan, S. Bao, J. Mi, B. B. Iversen, P. D. C. King, and Ph. Hofmann, *Nat. Commun.* **1**, 128 doi: 10.1038/ncomms1131 (2010).
- [15] R. C. Hatch, M. Bianchi, D. Guan, S. Bao, J. Mi, B. B. Iversen, L. Nilsson, L. Hornekær, and Ph. Hofmann, *Phys. Rev. B* **83**, 241303 (2011).
- [16] S. V. Hoffmann, C. Søndergaard, C. Schultz, Z. Li, and Ph. Hofmann, *Nuclear Inst. and Methods in Physics Research, A* **523**, 441 (2004).
- [17] Y. Xia, D. Qian, D. Hsieh, L. Wray, A. Pal, H. Lin, A. Bansil, D. Grauer, Y.S. Hor, R.J. Cava, and M. Z. Hasan, *Nat. Phys.* **5**, 398 (2009).
- [18] L.A. Wray, S.-Y. Xu, Y. Xia, Y.S Hor, D. Qian, A.V. Fedorov, H. Lin, A. Bansil, R.J. Cava, and M.Z. Hasan, *Nat. Phys.* **6**, 855 (2010).
- [19] [<http://www.flapw.de>]
- [20] D.M. Ceperley and B.J. Alder, *Phys. Rev. Lett.* **45**, 566 (1980) as parametrized by J.P. Perdew and A. Zunger, *Phys. Rev. B* **23**, 5048 (1981).
- [21] J.P. Perdew, K. Burke, and M. Ernzerhof, *Phys. Rev. Lett.* **77**, 3865 (1996); J.P. Perdew, K. Burke, and M. Ernzerhof, *Phys. Rev. Lett.* **78**, 1396(E) (1997).
- [22] C. Friedrich, S. Blügel, and A. Schindlmayr, *Phys. Rev. B* **81**, 125102 (2010).
- [23] See Supplemental Material at <http://link.aps.org/supplemental/XXX> for computational details and RPA results on the dielectric constant of bismuth selenide.
- [24] P. D. C. King, R. C. Hatch, M. Bianchi, R. Ovsyanikov, C. Lupulescu, G. Landolt, B. Slomski, J. H. Dil, D. Guan, J. L. Mi, E. D. L. Rienks, J. Fink, A. Lindblad, S. Svensson, S. Bao, G. Balakrishnan, B. B. Iversen, J. Osterwalder, W. Eberhardt, F. Baumberger, and Ph. Hofmann, *Phys. Rev. Lett.* **107**, 096802 (2011).
- [25] M. Bianchi, R. C. Hatch, J. Mi, B. B. Iversen, and Ph. Hofmann, *Phys. Rev. Lett.* **107**, 086802 (2011).
- [26] S. V. Eremeev, M. G. Vergniory, T. V. Menshchikova, A. A. Shaposhnikov, and E. V. Chulkov, *New Journal of Physics* (accepted)
- [27] T. V. Menshchikova, S. V. Eremeev, and E. V. Chulkov, *JETP Letters* **94**, 106 (2011).
- [28] M. Ye, S. V. Eremeev, K. Kuroda, M. Nakatake, S. Kim, Y. Yamada, E. E. Krasovskii, E. V. Chulkov, M. Arita, H. Miyahara, et al., *ArXiv* 1112.5869.
- [29] C. Chena, S. Hea, H. Wenga, W. Zhanga, L. Zhaoa, H. Liua, X. Jiaa, D. Moua, S. Liua, J. Hea, Y. Penga, Y. Fenga, Z. Xiea, G. Liua, X. Donga, J. Zhanga, X. Wangb, Q. Pengb, Z. Wangb, S. Zhangb, F. Yangb, C. Chenb, Z. Xub, X. Daia, Z. Fanga, and X. J. Zhoua, *PNAS* **109**, 3694 (2012).
- [30] M. Bianchi, R. C. Hatch, Zh. Li, Ph. Hofmann, F. Song, J. Mi, B. B. Iversen, Z. M. Abd El-Fattah, P. Löptien, L. Zhou, A. A. Khajetoorians, J. Wiebe, R. Wiesendanger, and J. W. Wells, *ACS Nano* **6**, 7009 (2012).